Tunable Metamaterial Devices by means of Two-Hot-Arm Electrothermal Actuators

A.X. LALAS, N.V. KANTARTZIS, T.V. YIOULTSIS, T.D. TSIBOUKIS

Department of Electrical and Computer Engineering, Aristotle University of Thessaloniki, GR-54124, Thessaloniki, Greece
E-mail: tsibukis@auth.gr

Abstract. A reconfigurable metamaterial, obtained from the combination of two-hot-arm electrothermal actuators with a split-ring resonator, is presented in this paper. Offer-ing a reliable control of the tip displacement, the selected actuators overcome the undesired bandwidth constraints of existing structures and establish significant levels of tunabil-ity. To this goal, the actuator is realized as an integrated part of the resonator. The proposed design is numerically verified through several setups which prove its left-handed behavior.

1. Introduction

Metamaterials, as artificially engineered electromag-netic media, exhibit unique electromagnetic properties not available in nature. Among the multitude of contemporary applications, their combination with nanostructures has been intensively researched [1]-[4]. Nonetheless, such implementations are still rather limited, mainly due to the lack of a wide spectral bandwidth. So, the design of meta-materials with a controllable operating frequency is deemed critical to overcome the prior constraints. To this aim, various tuning mechanisms have been proposed [5]-[8]. However, the excellent features of radio-frequency microelectromechanical systems (RF-MEMS) [9]-[11] offer the most viable solutions, as they introduce the de-sired tunability which circumvents bandwidth restrictions.

A noteworthy design of RF-MEMS switches that can provide robust control of the tip displacement, and hence fulfill the above requirements, is the two-hot-arm thermal actuator [12], [13]. This type of electrothermally actuated apparatus may be used as a powerful switching element or as a part of a tuning mechanism, *e.g.* a reconfigurable capacitor with an externally movable dielectric. In the former case, the actuator causes a negligible impact in the overall performance of the controllable device, while in the latter it is responsible only for the device's rear-rangement. Although various interesting studies have been presented, to the best of our knowledge, the association of the two-hot-arm thermal actuator with an electromag-netic structure as a fully operational component has not been yet numerically explored. Therefore, it is the goal of this paper to examine the combination of the aforemen-tioned actuator with a split-ring resonator (SRR) in order to obtain a reconfigurable metamaterial. The proposed design launches the actuator as an integral component of the SRR and supports its claims by a set of accurate nu-merical results with a left-handed profile.

2. Design of the Electrothermal Actuator

The two-hot-arm design approach of a thermal actuator exhibits some important advantages over existing realiza-tions, such as increased power consumption efficiency and thinner flexure, which lead to enhanced levels of deflection. Its principal operation is summarized in the asymmetric thermal expansion of the hot and cold arms, while an electric circuit is created by setting a potential difference between them. In this manner, electric current travels along the hot arms, resulting in resistive heating and thermal expansion, whereas the thicker arm remains cold, since it is not part of the electric circuit. Conse-quently, a deflection occurs owing to the expansion dif-ference between hot and cold arms.

The design parameters of the PolySilicon two-hot-arm horizontal thermal actuator, as depicted in Fig. 1, are: L_1 = 252 μm, L_2 = 220 μm, L_3 = 162 μm, L_4 = 38 μm, w_1 = 21 μm, w_2 = 14 μm, w_3 = 14 μm, d = 2 μm, and g = 5 μm. Also, the height of dimples and anchors is set to 2 μm, while the height of the remaining actuator is 2 μm.

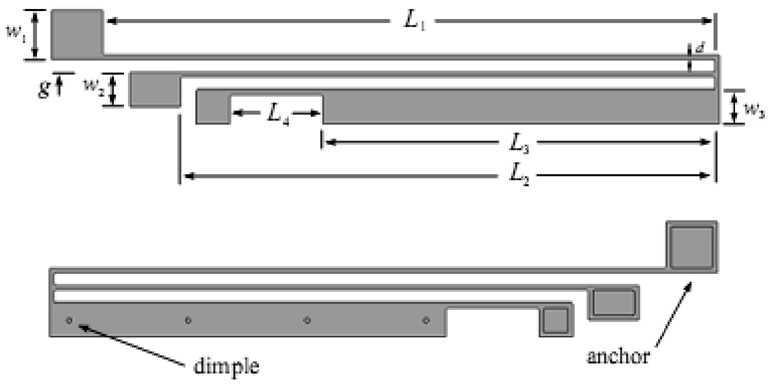

Fig. 1. Front and back side of the two-hot-arm actuator.

A cou-pled electric, thermal and structural analysis along with a parametric study for the actuation voltage are conducted in order to identify the primary characteristics of the device. In this framework, the displacement of the actuator's tip versus the actuation voltage is illustrated in Fig. 2.

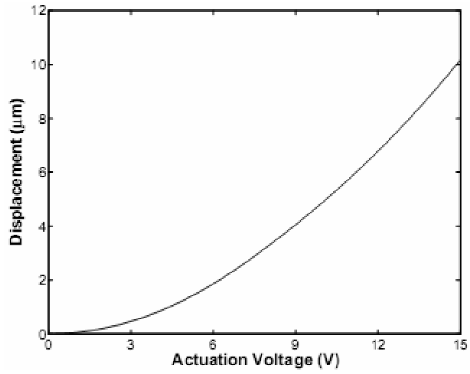

Fig. 2. Maximum tip displacement for different values of the actuation voltage.

To avoid the presence of unwanted short circuits that may degrade the device's performance, the operational range is limited to 15 V. Based on the above notions, Fig. 3 presents the deformed geometry of the actuator together with its corresponding total displacement distribution.

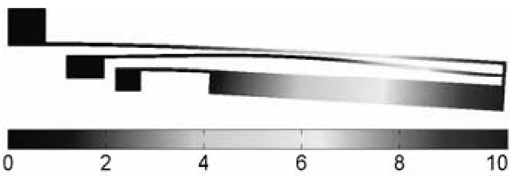

Fig. 3. Total displacement distribution on the actuator (in μm) at the actuation voltage of 15 V.

3. Controllable Metamaterial Unit Cell

The geometry of our controllable 550×473 μm meta-material unit cell – formed via the gap between the actua-tors and the SRR – is given in Fig. 4.

When a voltage is applied to the actuator's arms, a deformed structure oc-curs and the gap is shortened. Therefore, variations in voltage levels introduce a tunable gap and as a conse-quence a reconfigurable SRR. The width of its metal strip is 28 μm, the cell period is 650 μm, the height of the SRR is 4 μm, and the thickness of the Si_3N_4 substrate is 20 μm. Furthermore, the length and the width of the cou-pling bar between the two independent actuators are 150 μm and 14 μm, respectively. Bearing in mind the prior structural data, all numerical simulations are performed by means of the finite element method. In order to extract the S-parameters, a parallel-plate waveguide approach is adopted, which requires the use of PEC and PMC bound-ary conditions instead of the conventional periodic boundary conditions. Also, a robust homogenization method [14] is utilized to retrieve the constitutive effec-tive parameters of the proposed metamaterials. In this context, Fig. 5 illustrates the magnitude of the S_{11}- and S_{21}-parameter of the reconfigurable metamaterial at the actuator voltage of 0 V.

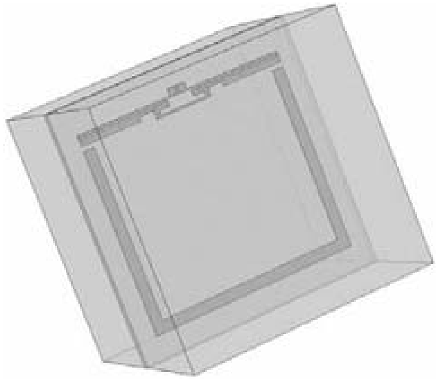

Fig. 4. Geometry of the electrothermally controlled, in terms of two independent actuators, metamaterial unit cell.

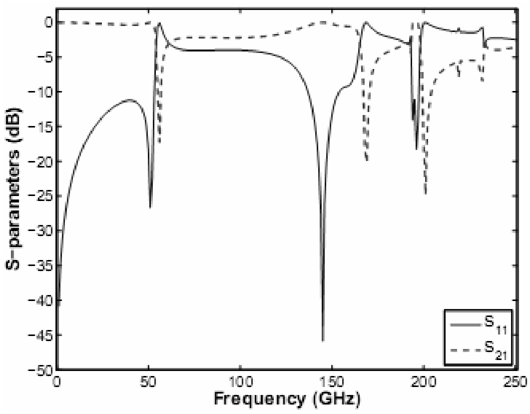

Fig. 5. S-parameters of the reconfigurable device at the ac-tuation voltage of 0 V.

Results indicate the pres-ence of three acute resonant frequencies for the S_{21}-parameter, *i.e*. at 56 GHz, 169 GHz, and 201 GHz. To this direction, the left-handed behavior of the combined structure can be substantiated in Fig 6, which illustrates the variation of the real and imaginary part of both effec-tive constitutive parameters.

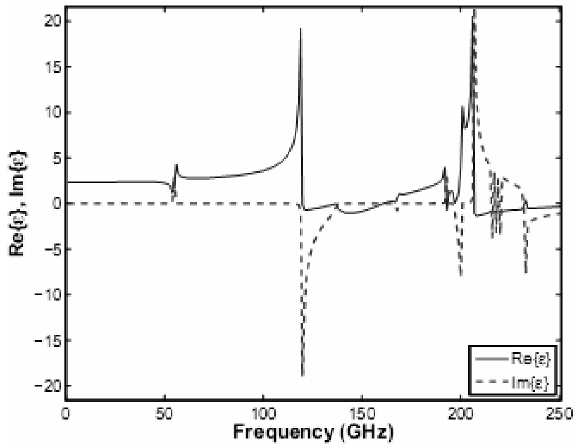

(a)

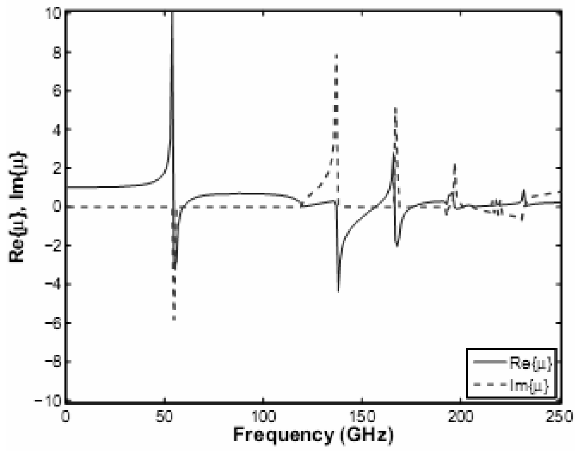

(b)

Fig. 6. Left-handed performance at the actuation voltage of 0 V. (a) Effective dielectric permittivity and (b) effective mag-netic permeability.

However, in order to ensure the validity of the homogenization technique the opera-tional wavelength must be higher than the cell period by a factor of 8 at least. Thus, the presence of three distinct negative μ frequency regions is easily discerned, but only the first is identified as a left-handed resonance. Additional evidence of the enhanced tunability accomplished by our controllable device can be obtained from Figs 7 and 8, where the variation of the S_{11}- and S_{21}-parameter is -l examined for different actuation voltages. In fact, as the actuation voltage increases from 0 V to 15 V, a certain shift (around 2-3 GHz) at all resonant frequencies is achieved.

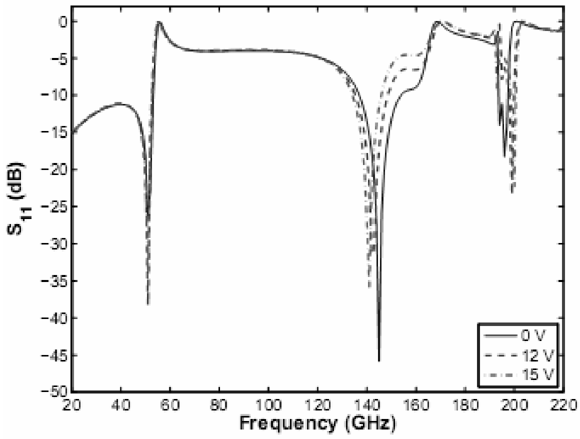

Fig. 7. Tunable behavior at several actuation voltages in terms of S_{11}-parameter.

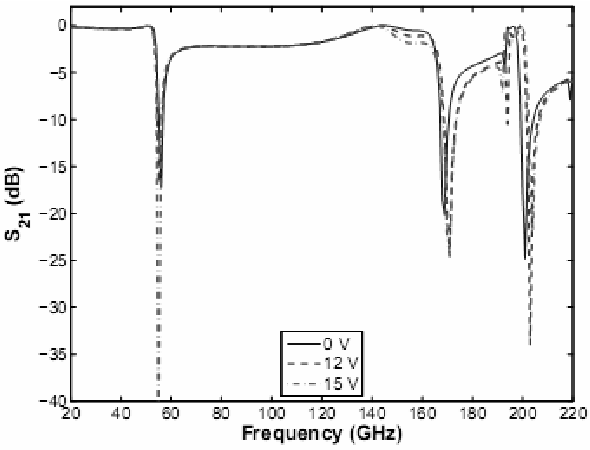

Fig. 8. Tunable behavior at several actuation voltages in terms of S_{21}-parameter.

Similar deductions may be drawn from the shift of the real part of the effective magnetic permeabil-ity in Fig. 9, while Fig. 10 presents two snapshots of the electric field at two resonant frequencies of the device for an actuation voltage of 0 V.

Concentrating on the results so far acquired, it has to be stressed that, despite initial theoretical predictions, a nontrivial number of multiple gaps is involved in the overall analysis. This simply implies that multiple reso-nant frequencies are sufficiently amplified, thus compli-cating the investigation of such devices. Moreover, it becomes apparent that the use of two independent electro-thermal actuators enables the fine tuning of the resulting metamaterial – with respect to the actuator voltage of 0 V– on condition that the proper bias network (separate for each actuator) is employed.

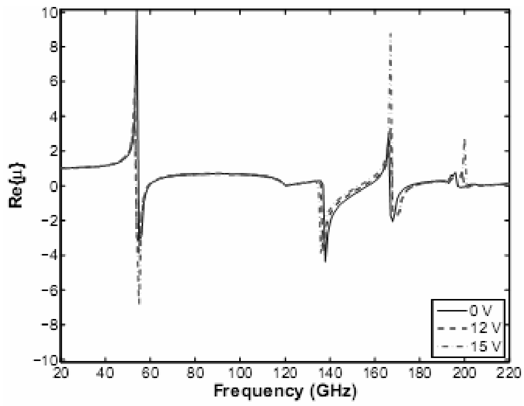

Fig. 9. Tunable left-handed performance at several actuation voltages in terms of effective magnetic permeability.

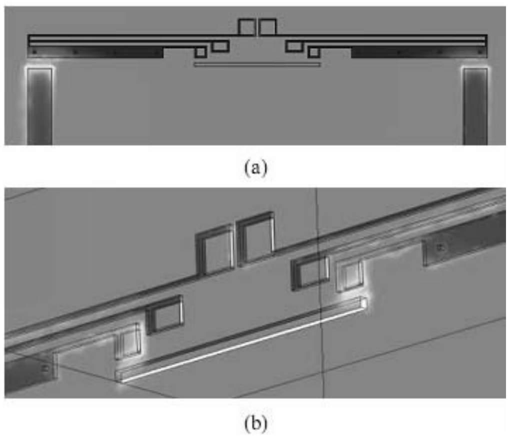

Fig. 10. Electric field snapshots of the electrothermally con-trolled, in terms of two independent actuators, metamaterial unit cell at (a) 56 GHz and (b) 201 GHz.

Should we have required a simpler configuration with only one bias network, the novel double parallel actuated structure of Fig. 11 can be considered. However, this simplification is at a slight expense of fine tunability, as the double parallel actuator is proven more rigid. So, this tradeoff between bias network complexity and fine tuna-bility must be taken into account during the design of such devices, depending on the operational priorities.

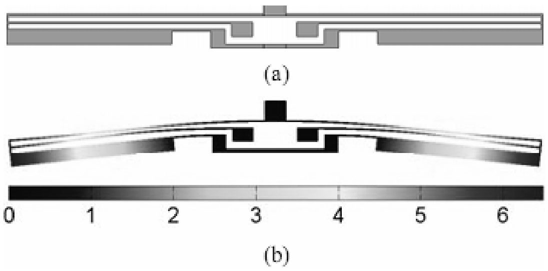

Fig. 11. (a) Geometry of the double parallel actuated device and (b) its total displacement distribution (in μm) at the actua-tion voltage of 12 V.

Taking into account the aforementioned properties, a reconfigurable metamaterial unit cell, which incorporates the double parallel actuated device, is designed and nu-merically investigated. The enhanced tunability achieved by our controllable device can be confirmed via Fig. 12, where the variation of the S_{11}- and S_{21}-parameter is exam-ined for different actuation voltages.

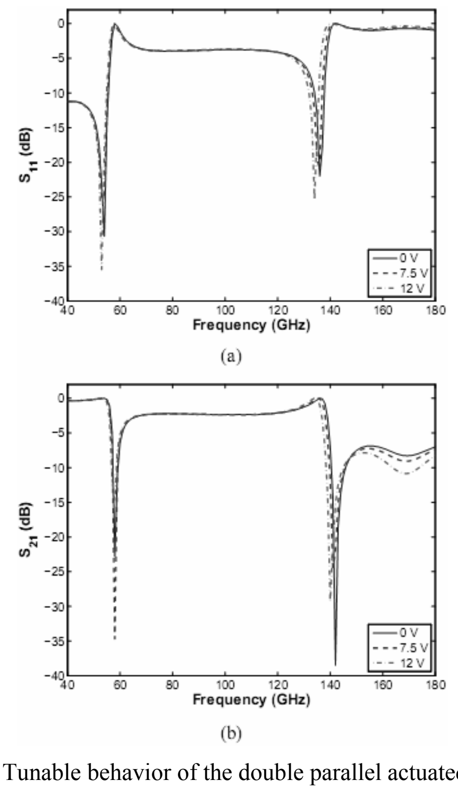

Fig. 12. Tunable behavior of the double parallel actuated de-vice at several actuation voltages in terms of (a) S_{11}-parameter and (b) S_{21}-parameter.

At 0 V, the presence of two acute resonant frequencies for the S_{21}-parameter, *i.e*. at 58 GHz and 142 GHz, is revealed. However, as the actuation voltage increases from 0 V to 12 V, a certain shift (around 1-2 GHz) at all resonant frequencies is observed. Congruent deductions may be obtained from the shift of the real part of the effective magnetic perme-ability in Fig. 13, while the homogenization condition, denoting a left-handed performance, is only satisfied for the first resonance. Finally, Fig. 14 presents a snapshot of the electric field at the first resonant frequency of the device for an actuation voltage of 12 V.

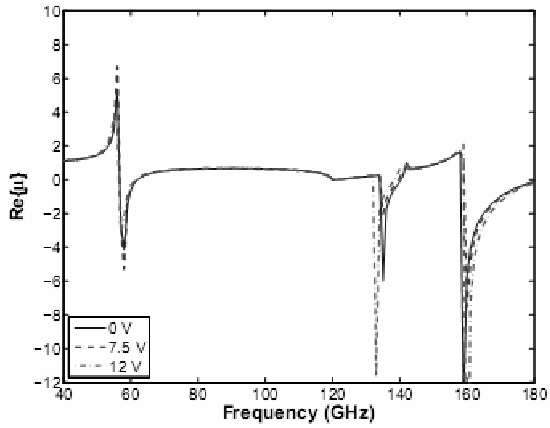

Fig. 13. Tunable left-handed performance of the double parallel actuated device at several actuation voltages in terms of effective magnetic permeability.

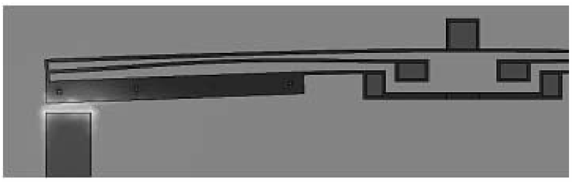

Fig. 14. Electric field snapshot of the double parallel actuated device at 58 GHz.

The reconfigurable unit cells presented herein exhibit left-handed behavior as well as conventional performance depending on the frequency region utilized. In both cases, the tuning property in terms of bandwidth and frequency shifting is accomplished, thus allowing the design of sev-eral applications, such as millimeter wave filters and modulators. Moreover, the electrothermal principle of controllability provided by the two-hot-arm horizontal thermal actuator enables driving these devices by means of a low voltage. Hence, the controllable unit cells may be incorporated in mobile apparatus, where low voltage specifications are enforced by limited power availability.

4. Conclusion

The use of two-hot-arm thermal actuators in the effi-cient design of finely tunable metamaterials has been analyzed and numerically studied in this paper. A left-handed performance has been attained for several states, leading to useful millimeter wave implementations.

Acknowledgement. This work was supported by the National Scolarships Foundation of Greece (IKY), under Grant No. 5282.

References

[1] J.F. O'HARA, R. SINGH, I. BRENER, *et al.*, *Thin-film sensing with planar terahertz metamaterials: sensitivity and limita-tions*, Opt. Express, **16**, pp. 1786–1795, 2008.

[2] L. SOLYMAR and E. SHAMONINA, Waves in Metamaterials, 1st ed., Oxford University Press, Inc., 2009.

[3] A.E. NIKOLAENKO, F. DE ANGELIS, S.A. BODEN, *et al.*, *Car-bon nanotubes in a photonic metamaterial*, Physical Re-view Letters, **104**, art. no. 153902(1-4), 2010.

[4] R. SINGH, I.A.I. AL-NAIB, M. KOCH and W. ZHANG, *Asymmetric planar terahertz metamaterials*, Opt. Ex-press, **18**, pp. 13044–13050, 2010.

[5] H. TAO, A.C. STRIKWERDA, K, FAN, *et al.*, *Reconfigurable terahertz metamaterials*, Phys. Rev.Lett. **103**, 147401, 2009.

[6] J.M. MANCEAU, N.H. SHEN, M. KAFESAKI, *et al.*, *Dynamic response of metamaterials in the terahertz regime: Blue-shift tunability and broadband phase modulation*, Appl. Phys. Lett. **96**, 021111, 2010.

[7] W.M. ZHU, H. CAI, T. BOUROUINA, *et al.*, *A MEMS tunable metamaterial filter*, in Proceedings of the 23rd Interna-tional Conference on MEMS, pp. 196–199, Hong Kong, China, January 2010.

[8] X.-J. HE, Y. WANG, J.-M. WANG and T.-L. GUI, *MEMS switches controlled multi-split ring resonator as a tunable metamaterial component*, Microsystem Technology, **16**, pp. 1831–1837, 2010.

[9] G.M. REBEIZ, *RF MEMS: Theory, Design, and Technol-ogy*, 1st ed., John Wiley & Sons, Inc., 2003.

[10] C. LUGO, G. WANG, J. PAPAPOLYMEROU, *et al.*, *Frequency and bandwidth agile millimeter-wave filter using ferroelec-tric capacitors and MEMS cantilevers*, IEEE Transactions on Microwave Theory and Techniques, **55**(2), pp. 376–382, 2007.

[11] S. LUCYSZYN (Ed.), Advanced RF MEMS, 1st ed., Cam-bridge University Press, 2010.

[12] D. YAN, A. KHAJEPOUR and R. MANSOUR, *Modeling of two-hot-arm horizontal thermal actuator*, Journal of Microme-chanics and Microengineering, **13**, pp. 312–322, 2003.

[13] D. GIRBAU, M. LLAMAS, *et al.*, *A low-power-consumption out-of-plane electrothermal actuator*, Journal of Micro-electromechanical Systems, **16**, pp. 719–727, 2007.

[14] X. CHEN, T.M. GRZEGORCZYK, B.I. WU, J. PACHECO and J.A. KONG, *Robust method to retrieve the constitutive ef-fective parameters of metamaterials*, Physical Review E, **70**(1), art. no. 016608(1–7), 2004.